# Recent results of heavy flavor and CPV at ATLAS

Yue Xu

*On behalf of the ATLAS Collaboration*

Tsinghua University

HFCPV2022

11 December, 2022

# The ATLAS detector

- ATLAS (A Toroidal LHC ApparatuS) is one of the two general-purpose detectors at the Large Hadron Collider (LHC)
  - Coverage: $|\eta| < 2.5$
  - Magnetic field: 2T
- Excellent track and muon identification with the goodness of the inner detector and muon spectrometer.

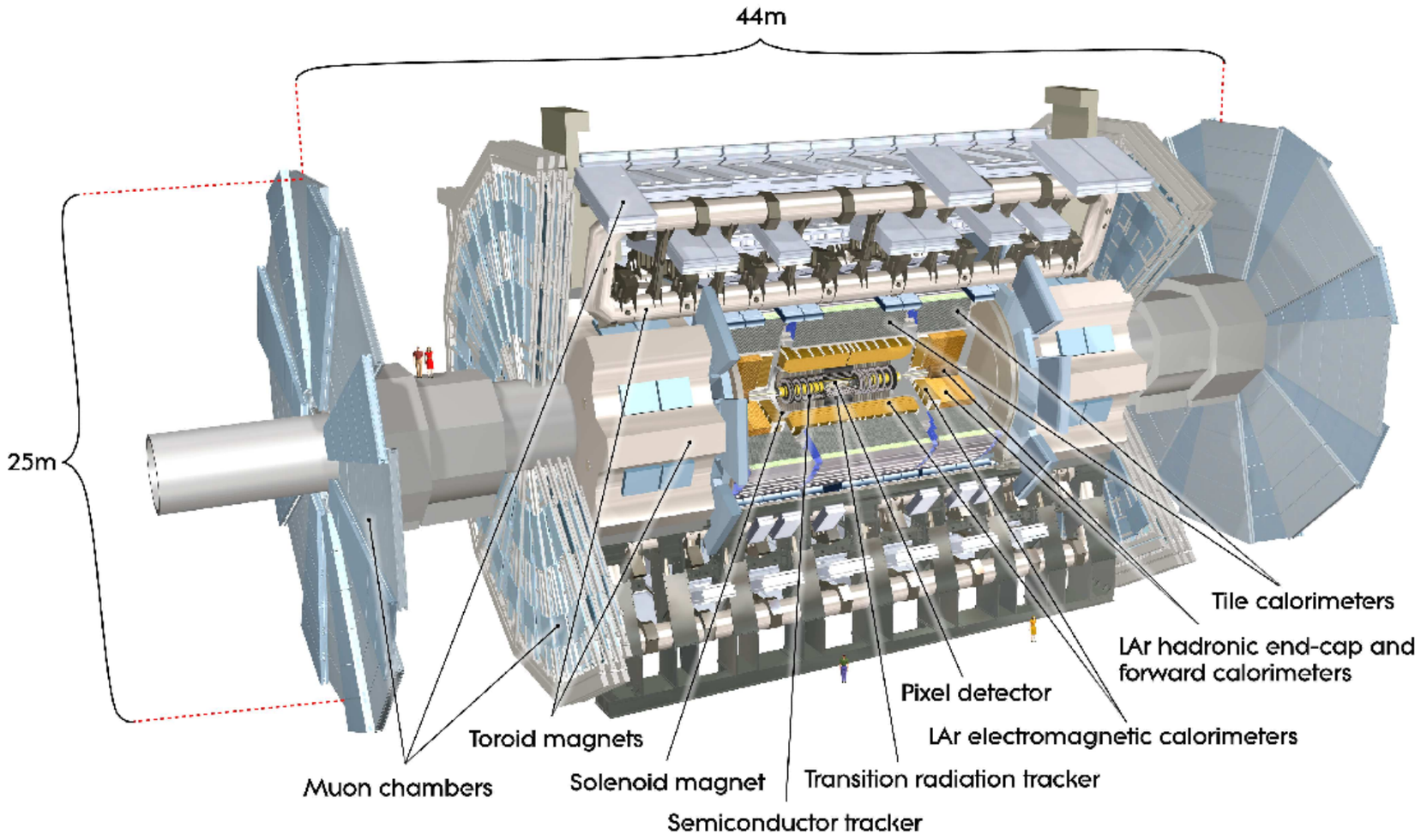

# Outline

- Observation of an excess of di-charmonium events in the four-muon final state at $\sqrt{s} = 13$ TeV with the ATLAS detector (2015-2018) ATLAS-CONF-2022-040
- Measurement of the CP-violation phase $\phi_s$ in $B_s^0 \to J/\psi\phi$ decays in ATLAS at 13 TeV (2015-2017) Eur. Phys. J. C 81 (2021) 342

- Observation of an excess of di-charmonium events in the four-muon final state with the ATLAS detector (2015-2018) ATLAS-CONF-2022-040

- Measurement of the CP-violation phase $\phi_s$ in $B_s^0 \to J/\psi\phi$ decays in ATLAS at 13 TeV (2015-2017) Eur. Phys. J. C 81 (2021) 342

# X(6900) from LHCb

- At June 2020, LHCb claimed evidence for a narrow resonance in the di-$J/\psi$ to 4 muons spectrum at **6.9 GeV**, presumably coming from 4-charm quark state.

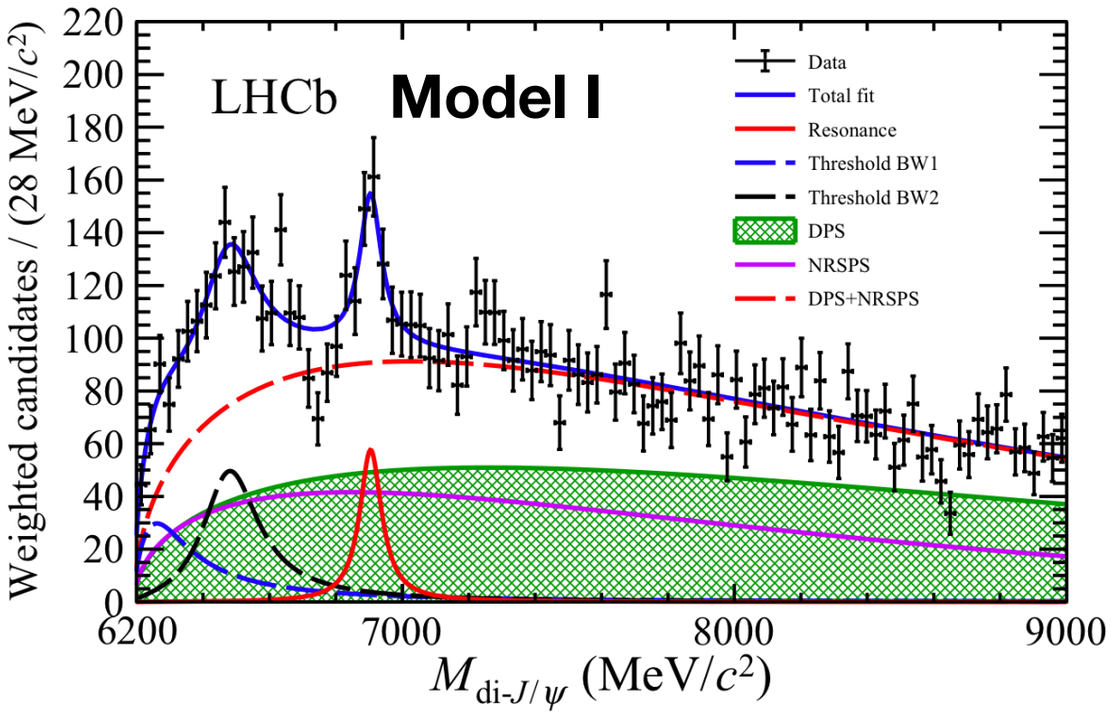


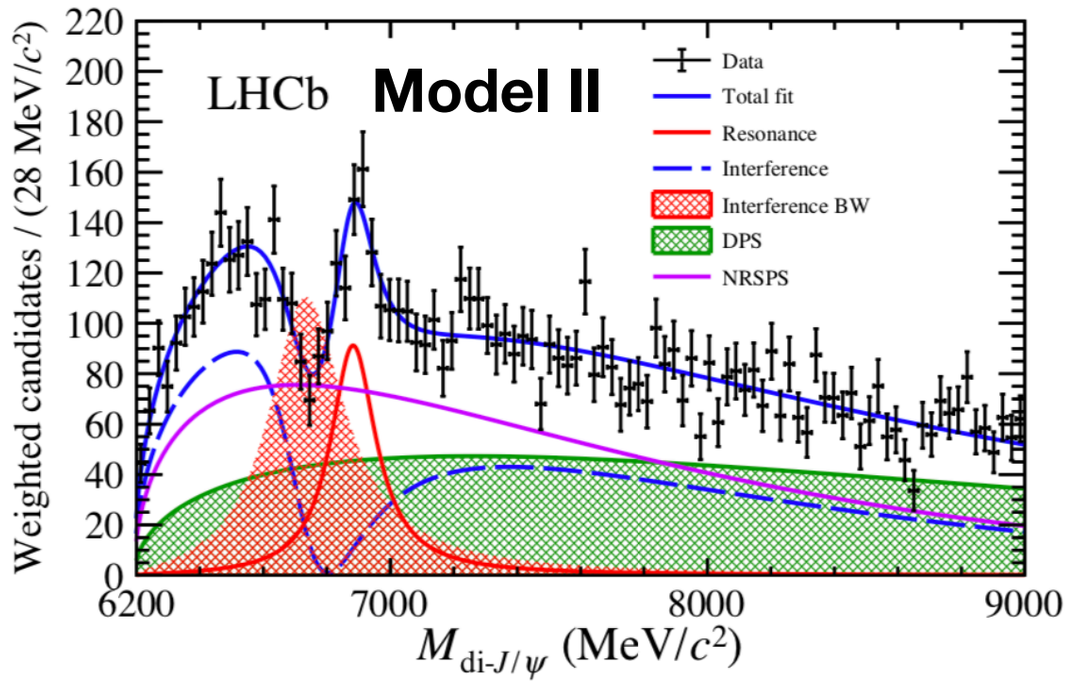


arXiv:2006.16957

| | |
|---|---|
| LHCb model I: no interference | $m[X(6900)] = 6905 \pm 11 \pm 7\,\text{MeV}/c^2$<br>$\Gamma[X(6900)] = 80 \pm 19 \pm 33\,\text{MeV}$ |
| LHCb model II: interference | $m[X(6900)] = 6886 \pm 11 \pm 11\,\text{MeV}/c^2$<br>$\Gamma[X(6900)] = 168 \pm 33 \pm 69\,\text{MeV}$ |

# Data, Signal and backgrounds

- Data: $139$ fb$^{-1}$ @ 13 TeV in 2015-2018.

- **Signal** process: tetraquark (TQ)
  $\rightarrow J/\psi + J/\psi$ or $J/\psi + \psi(2S) \rightarrow 4\mu$

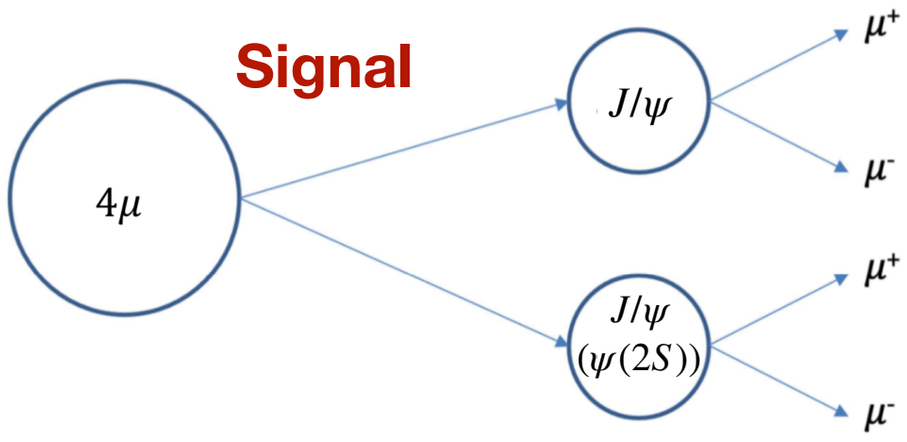


- Backgrounds:

- **Single parton scattering (SPS)**

- **Double parton scattering (DPS)**

- **Non-prompt** ( $b\bar{b} \rightarrow J/\psi + J/\psi/\psi(2S) + X \rightarrow 4\mu$)

- Single $J/\psi$ background and non-peaking background containing no real $J/\psi$ candidate (**Others)**

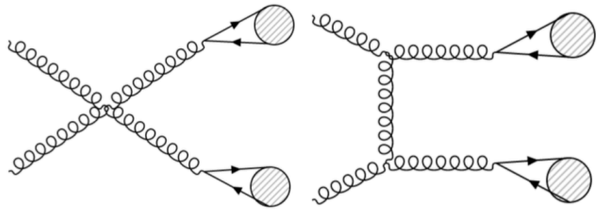


SPS

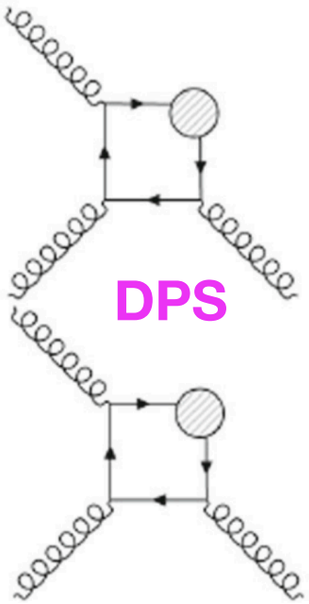


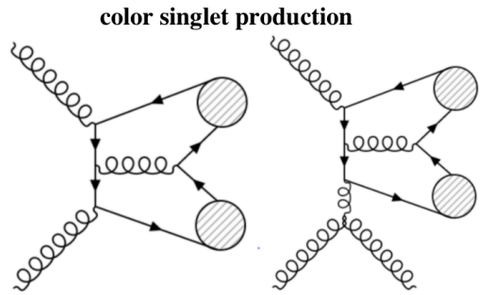

# Event selection and analysis regions

- Two positive charged muons and two negative charged muons:
  - $p_T(\mu_1) > 4$, $p_T(\mu_2) > 4$, $p_T(\mu_3) > 3$, $p_T(\mu_4) > 3$ GeV and $|\eta_{\mu_1,\,\mu_2,\,\mu_3,\,\mu_4}| < 2.5$
- Signal region (SR) is used to extract signal parameters (e.g. mass, width).
- SPS and DPS control regions (CR) are used to estimate SPS and DPS backgrounds.
- Non-prompt region is used to validate non-prompt background estimation.

| | | |
|---|---|---|
| **SR** | Tight vertex cuts:<br>$\lvert L_{xy}^{di-\mu} \rvert < 0.3$ mm<br>$L_{xy}^{4\mu} < 0.2$ mm<br>$\chi^2_{4\mu}/N < 3$ | $m_{4\mu} < 7.5$ GeV,<br>$\Delta R < 0.25$ between charmonia |
| **SPS CR** | | $7.5$ GeV $< m_{4\mu} < 12.0$ GeV |
| **DPS CR** | | $14.0$ GeV $< m_{4\mu} < 25.0$ GeV |
| **Non-prompt region** | Reverse vertex cuts: $\chi^2_{4\mu}/N > 6$ and $\lvert L_{xy}^{di-\mu} \rvert > 0.4$ mm | |

# Fit models

- Unbinned maximum likelihood fits are performed to extract the signal parameters (e.g. mass m, width $\Gamma$)
- Fit regions:
  - Fit SR: $m_{4\mu}^{\text{con}} < 11$ GeV and $\Delta R < 0.25$
  - Fit CR: $m_{4\mu}^{\text{con}} < 11$ GeV and $\Delta R \geq 0.25$, for SPS shape validation

**with a $J/\psi$ or $\psi(2S)$ mass constraint**

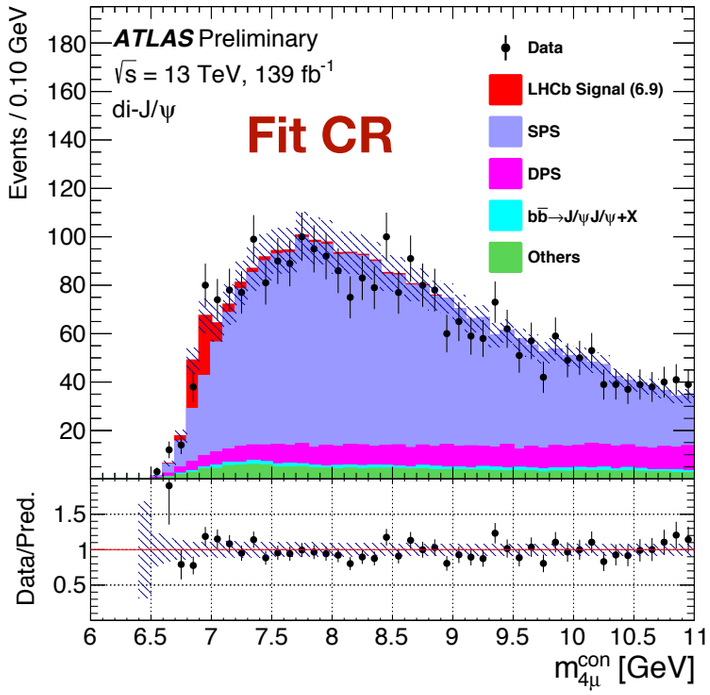


- In di-$J/\psi$ channel, **3-peak model** with interference among signals is considered. 2-peak model is also tested but with worse fit quality.

$$f_s(x) = \left| \sum_{i=0}^{2} \frac{z_i}{x^2 - m_i^2 + i m_i \Gamma_i} \right|^2 \sqrt{1 - \frac{4m_{J/\psi}^2}{x^2}} \otimes R(\alpha)$$

**Resolution function**

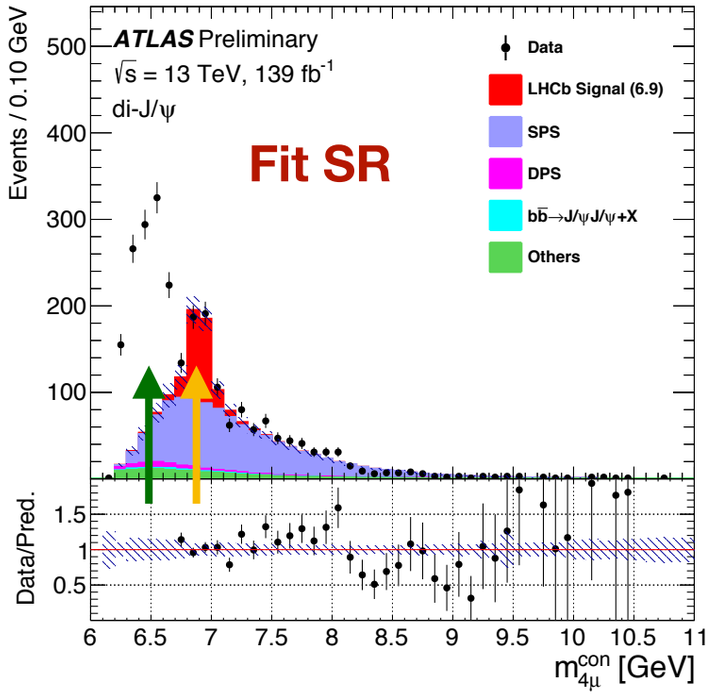

# Fit models

- In $J/\psi + \psi(2S)$ channel, due to lower statistics, two models are considered.
  - Model A: the same peaks with interference observed in the di-$J/\psi$ channel also decaying into $J/\psi + \psi(2S)$ plus a standalone peak.

$$f_s(x) = \left( \left| \sum_{i=0}^{2} \frac{z_i}{x^2 - m_i^2 + i m_i \Gamma_i} \right|^2 + \left| \frac{z_3}{x^2 - m_3^2 + i m_3 \Gamma_3} \right|^2 \right) \sqrt{1 - \left( \frac{m_{J/\psi} + m_{\psi(2S)}}{x} \right)^2} \otimes R(\alpha)$$

  - Model B: only one single peak

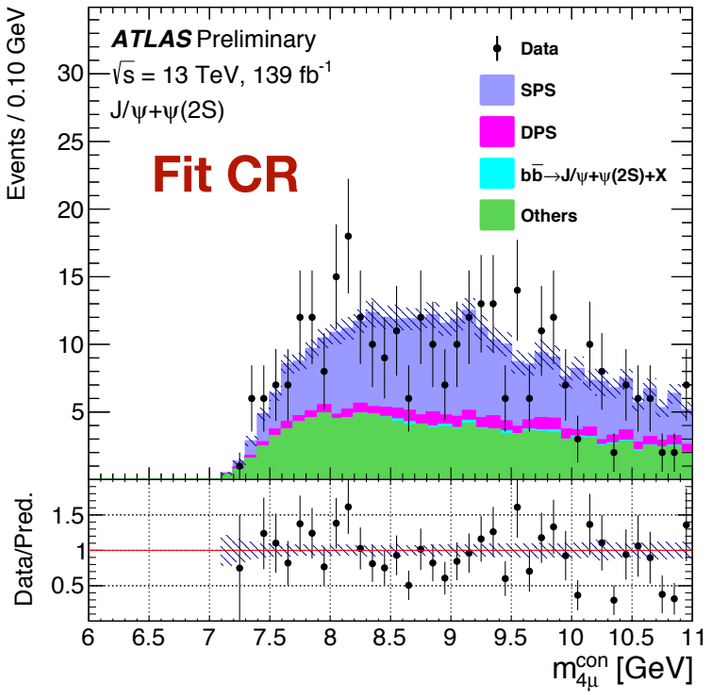


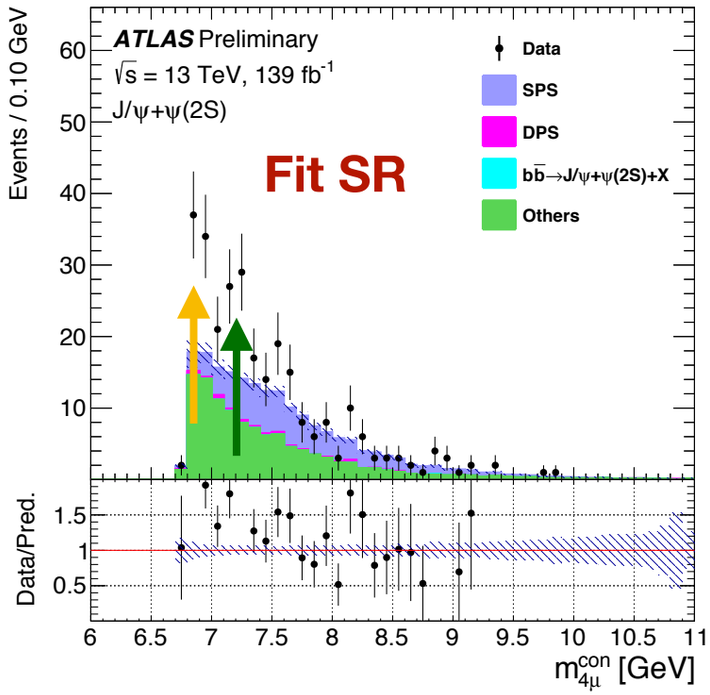

# Fit results in di-$J/\psi$ channel

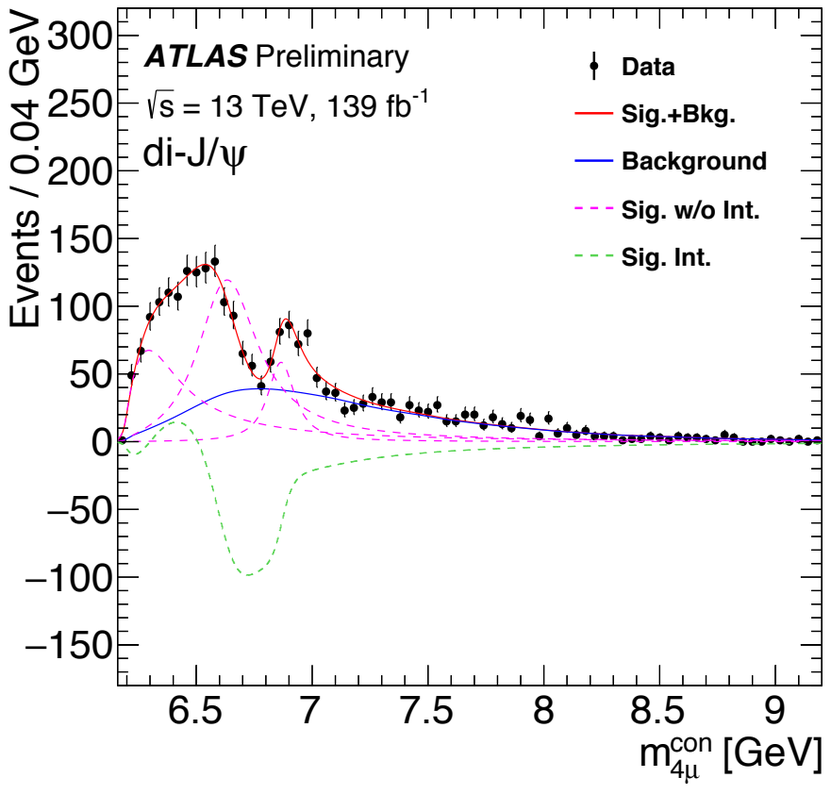


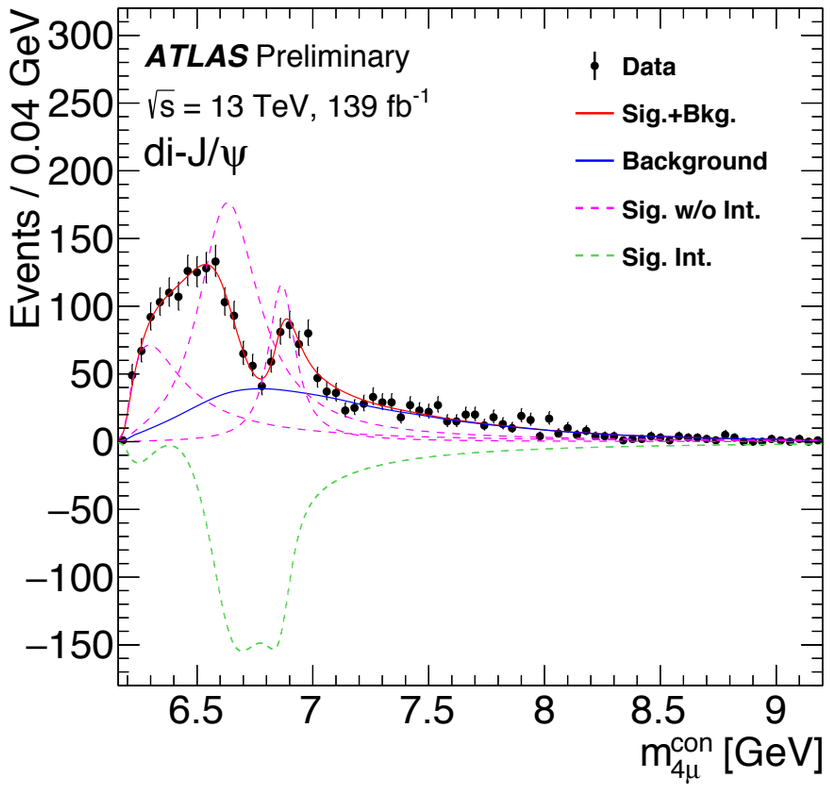


- The **3rd peak** mass is consistent with the LHCb observed X(6900), with significance of **10$\sigma$**
- The broad structure at the lower mass could from other physical effects, e.g. feed-down from higher di-charmonium resonances

**Extracted masses and widths (GeV)**

| (GeV) | $m_0$ | $\Gamma_0$ | $m_1$ | $\Gamma_1$ |
|---|---|---|---|---|
| di-$J/\psi$ | $6.22 \pm 0.05^{+0.04}_{-0.05}$ | $0.31 \pm 0.12^{+0.07}_{-0.08}$ | $6.62 \pm 0.03^{+0.02}_{-0.01}$ | $0.31 \pm 0.09^{+0.06}_{-0.11}$ |
| | $m_2$ | $\Gamma_2$ | — | |
| | $6.87 \pm 0.03^{+0.06}_{-0.01}$ | $0.12 \pm 0.04^{+0.03}_{-0.01}$ | — | |

# Fit results in $J/\psi + \psi(2S)$channel

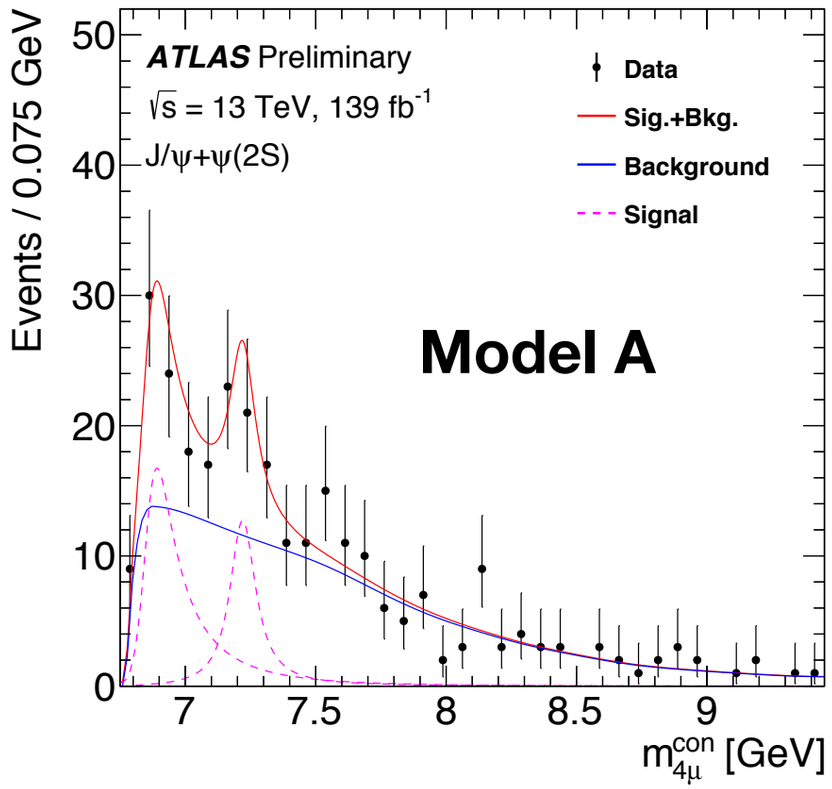


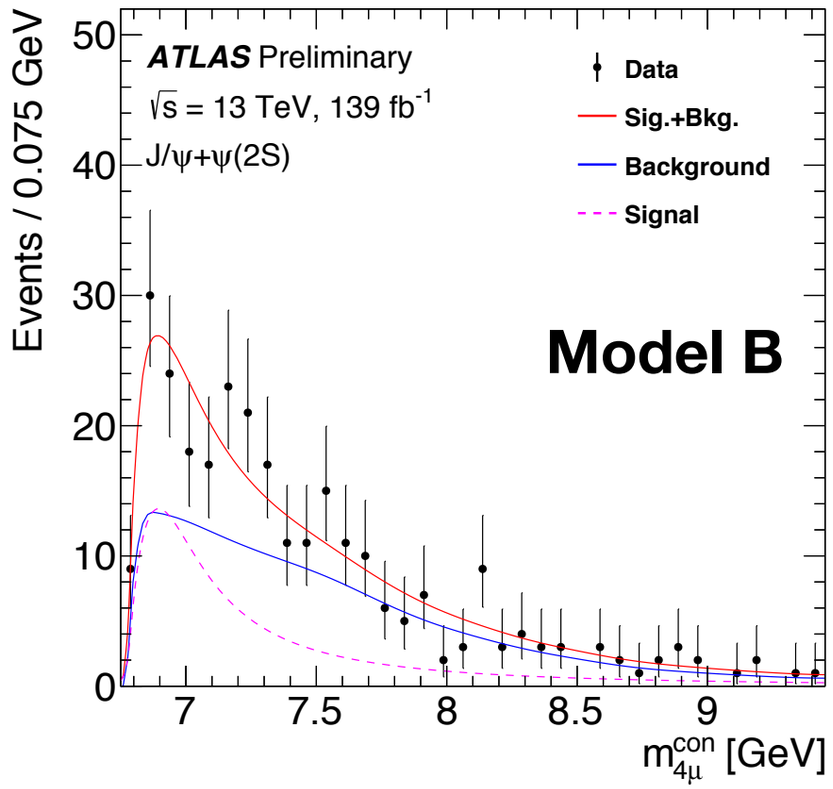


**Extracted masses and widths (GeV)**

| (GeV) | | $m_3$ | $\Gamma_3$ |
|---|---|---|---|
| $J/\psi+\psi(2S)$ | model A | $7.22 \pm 0.03^{+0.02}_{-0.03}$ | $0.10^{+0.13+0.06}_{-0.07-0.05}$ |
| | model B | $6.78 \pm 0.36^{+0.35}_{-0.54}$ | $0.39 \pm 0.11^{+0.11}_{-0.07}$ |

- In model A, the 1st peak could be related to X(6900) in the di-$J/\psi$ channel. The significance of **2nd peak** (7.2 GeV) reaches $3.2\sigma$, also hinted by LHCb in the di-$J/\psi$ spectrum

# Uncertainties

| Systematics (MeV) | di-$J/\psi$ | | | | | | $J/\psi$+$\psi$(2S) | |
|---|---|---|---|---|---|---|---|---|
| | $m_0$ | $\Gamma_0$ | $m_1$ | $\Gamma_1$ | $m_2$ | $\Gamma_2$ | $m_3$ | $\Gamma_3$ |
| SPS theory | 7 | 15 | 4 | 20 | 5 | 6 | <1 | |
| SPS di-charmonium $p_T$ | <1 | 8 | 4 | 14 | 5 | 7 | <1 | |
| Background MC statistics | <1 | 8 | 4 | 14 | 5 | 7 | <1 | |
| Mass resolution | 19 | 34 | 3 | 21 | 4 | 9 | <1 | 4 |
| Fit bias | 43 | 58 | 10 | 56 | 11 | 16 | 13 | 41 |
| Nonclosure | | | <1 | | | | <1 | |
| Transfer factor | | | — | | | | <1 | 16 |
| Presence of fourth peak | 29 | 49 | 11 | 108 | 60 | 18 | — | |
| Interference of fourth peak | | | — | | | | 29 | 11 |
| Data statistics | 50 | 119 | 34 | 88 | 30 | 39 | 28 | 130 |

- Data statistics has the largest impact in both two channels, followed by the systematic uncertainty from impact of fourth peak

- Observation of an excess of di-charmonium events in the four-muon final state with the ATLAS detector (2015-2018) ATLAS-CONF-2022-040

- Measurement of the CP-violation phase $\phi_s$ in $B_s^0 \to J/\psi\phi$ decays in ATLAS at 13 TeV (2015-2017) Eur. Phys. J. C 81 (2021) 342

# Introduction

- In the presence of new physics phenomena, additional sources of *CP* violation in *b*-hadron decays can arise.

- This analysis studies the $B_s^0 \to J/\psi(\mu^+\mu^-)\phi(K^+K^-)$decay. The CP violation occurs due to interference between a direct decay and a decay from $B_s^0 - \bar{B}_s^0$ mixing.

- CP violation phase $\phi_s$ : the weak phase difference between the $B_s^0 - \bar{B}_s^0$ mixing amplitude and the $b \to c\bar{c}s$ decay amplitude.

- In Standard Model, $\phi_s \approx -2\beta_s = -0.03696^{+0.00072}_{-0.00082}$ rad [CKMFitter]

Physical parameters:

- $\phi_s$
- Average decay width $\Gamma_s$
- Width difference $\Delta\Gamma_s$

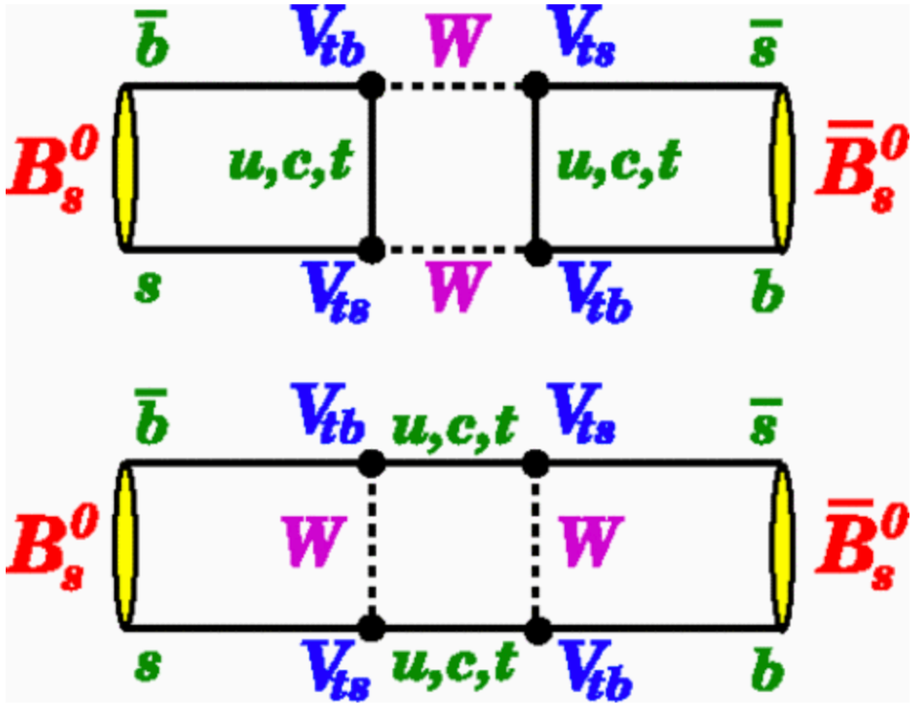


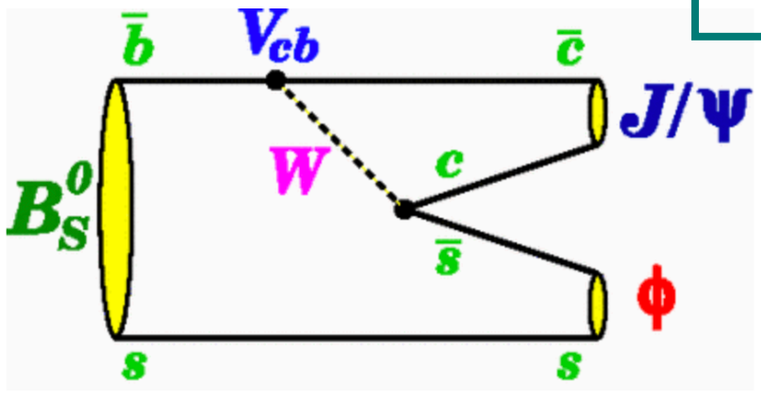


Phys. Rev. D 85, 072002

# Flavour tagging

- Tag flavour of the signal B meson using the opposite b-hadron produced from the pair production of $b$ and $\bar{b}$ quarks.

- "Cone charge" ($Q_x$) is defined as $p_T$ weighted sum of charge in a cone of size $\Delta R$, which provides strong discrimination power.

$$Q_x = \frac{\sum_i^{N\ \text{tracks}} q_i \cdot (p_{\mathrm{T}i})^\kappa}{\sum_i^{N\ \text{tracks}} (p_{\mathrm{T}i})^\kappa}$$

- **Muon (electron)-based tagging**: semileptonic decay of a B meson; $\kappa = 1.1\ (1.0)$ and $\Delta R = 0.5$

- **Jet tagging**: in the absence of a muon or electron; $\kappa = 1.1$ and $\Delta R = 0.5$

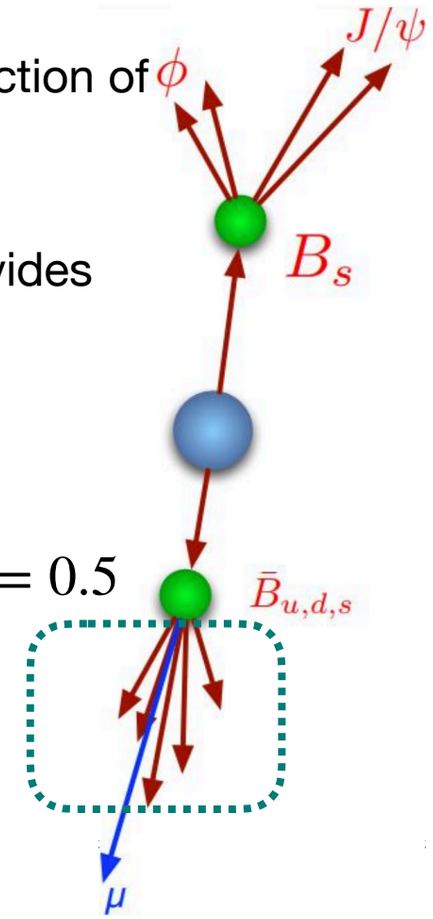


- Taggers are calibrated and optimized by self-tagging $B^\pm \to J/\psi K^\pm$ channel

- Classify taggers by efficiency ($\epsilon_x$), dilution ($D_x$) and tagging power ($T_x$).

| Tag method | $\epsilon_x$ (%) | $D_x$ (%) | $T_x$ (%) |
|---|---|---|---|
| Tight muon | $4.50 \pm 0.01$ | $43.8 \pm 0.2$ | $0.862 \pm 0.009$ |
| Electron | $1.57 \pm 0.01$ | $41.8 \pm 0.2$ | $0.274 \pm 0.004$ |
| Low-$p_{\mathrm{T}}$ muon | $3.12 \pm 0.01$ | $29.9 \pm 0.2$ | $0.278 \pm 0.006$ |
| Jet | $12.04 \pm 0.02$ | $16.6 \pm 0.1$ | $0.334 \pm 0.006$ |
| Total | $21.23 \pm 0.03$ | $28.7 \pm 0.1$ | $1.75 \pm 0.01$ |

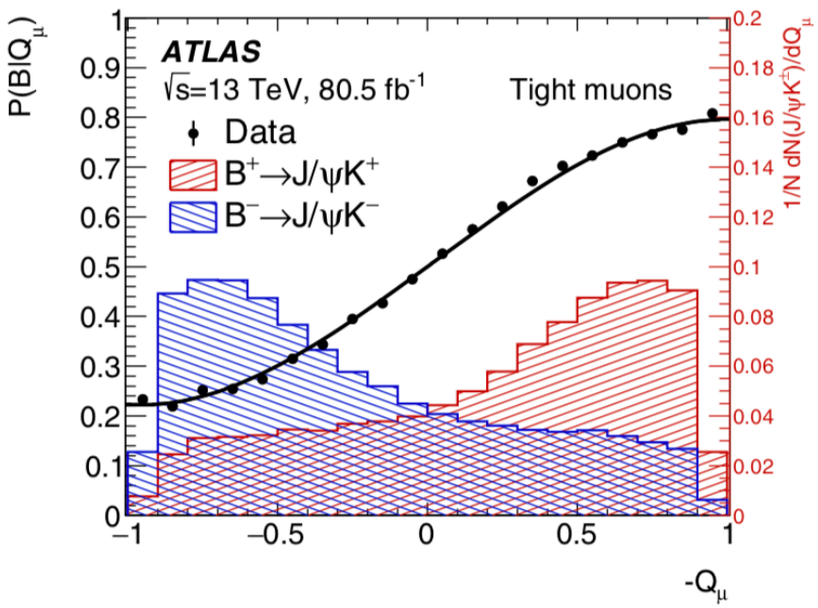

# Fit to data

- Data: $80.5$ fb$^{-1}$ @ 13 TeV in 2015-2017.
- An unbinned maximum likelihood fit is performed with a combination of signal and background probability density functions (PDFs).
- A time-dependent angular analysis is required to untangle CP-even and odd states.

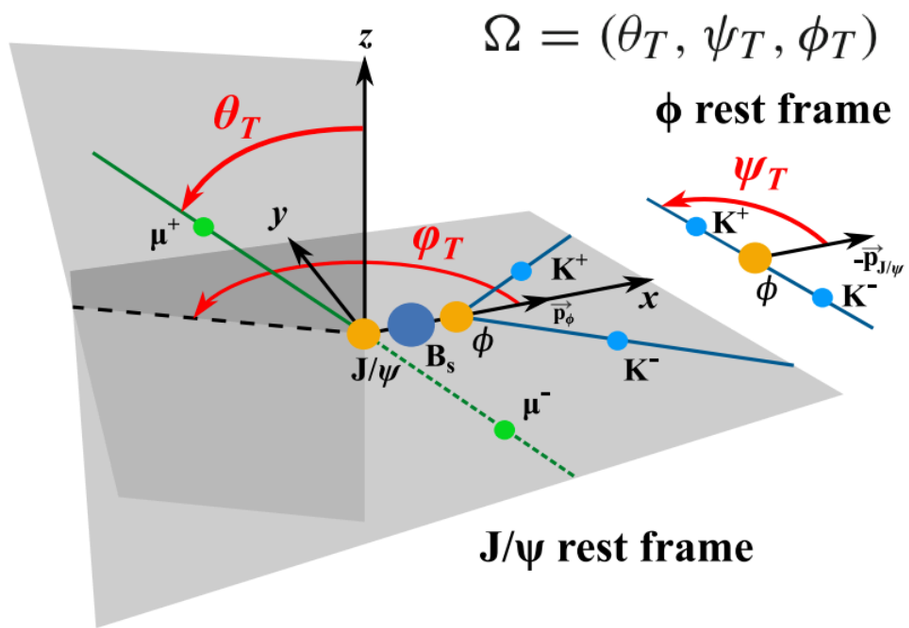


$$\ln \mathcal{L} = \sum_{i=1}^{N} w_i \cdot \ln[ f_{\mathrm{s}} \cdot \mathcal{F}_{\mathrm{s}}(m_i, t_i, \sigma_{m_i}, \sigma_{t_i}, \Omega_i, P_i(B|Q_x), p_{\mathrm{T}_i})$$
$$+ f_{\mathrm{s}} \cdot f_{B^0} \cdot \mathcal{F}_{B^0}(m_i, t_i, \sigma_{m_i}, \sigma_{t_i}, \Omega_i, P_i(B|Q_x), p_{\mathrm{T}_i})$$
$$+ f_{\mathrm{s}} \cdot f_{\Lambda_b} \cdot \mathcal{F}_{\Lambda_b}(m_i, t_i, \sigma_{m_i}, \sigma_{t_i}, \Omega_i, P_i(B|Q_x), p_{\mathrm{T}_i})$$
$$+ (1 - f_{\mathrm{s}} \cdot (1 + f_{B^0} + f_{\Lambda_b}))\mathcal{F}_{\mathrm{bkg}}(m_i, t_i, \sigma_{m_i}, \sigma_{t_i},$$
$$\Omega_i, P_i(B|Q_x), p_{\mathrm{T}_i})],$$

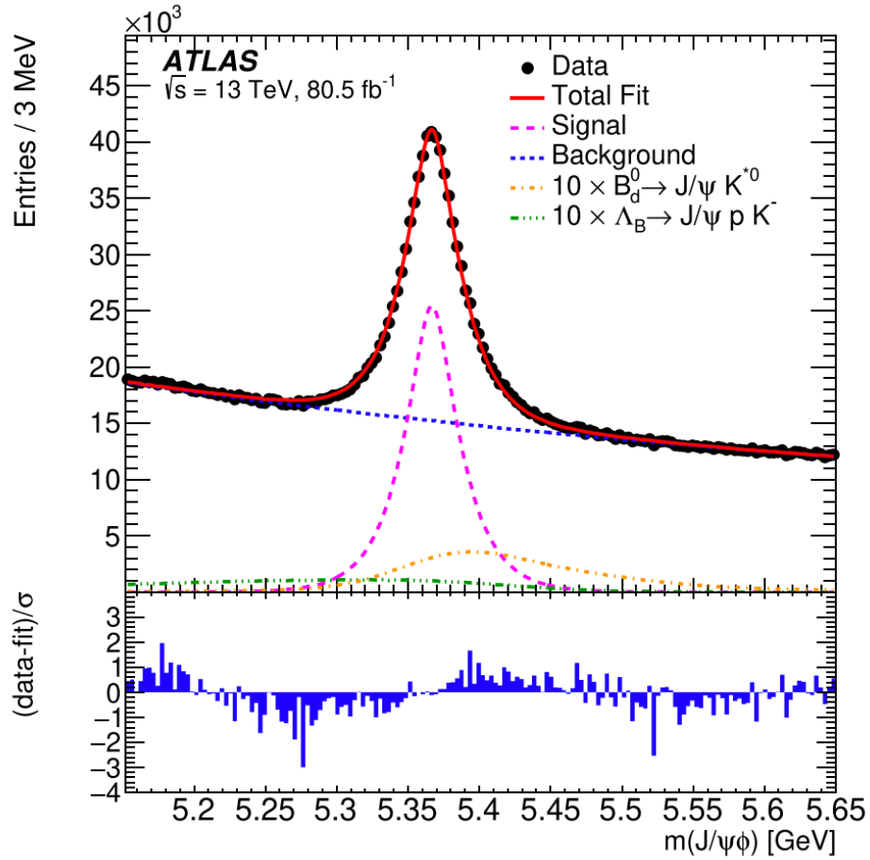

# Fit results

- The measurement of $\phi_s$ is consistent with the SM prediction.

- Contours of 68% confidence level are set in the $\phi_s - \Delta\Gamma_s$ plane. The results are consistent with the Run1 results, and improves the precision of previous ATLAS measurements.

| Parameter | Value | Statistical uncertainty | Systematic uncertainty |
|---|---|---|---|
| $\phi_s$ [rad] | −0.081 | 0.041 | 0.022 |
| $\Delta\Gamma_s$ [ps$^{-1}$] | 0.0607 | 0.0047 | 0.0043 |
| $\Gamma_s$ [ps$^{-1}$] | 0.6687 | 0.0015 | 0.0022 |
| $\lvert A_\parallel(0)\rvert^2$ | 0.2213 | 0.0019 | 0.0023 |
| $\lvert A_0(0)\rvert^2$ | 0.5131 | 0.0013 | 0.0038 |
| $\lvert A_S(0)\rvert^2$ | 0.0321 | 0.0033 | 0.0046 |
| $\delta_\perp - \delta_S$ [rad] | −0.25 | 0.05 | 0.04 |
| Solution (a) | | | |
| $\delta_\perp$ [rad] | 3.12 | 0.11 | 0.06 |
| $\delta_\parallel$ [rad] | 3.35 | 0.05 | 0.09 |
| Solution (b) | | | |
| $\delta_\perp$ [rad] | 2.91 | 0.11 | 0.06 |
| $\delta_\parallel$ [rad] | 2.94 | 0.05 | 0.09 |

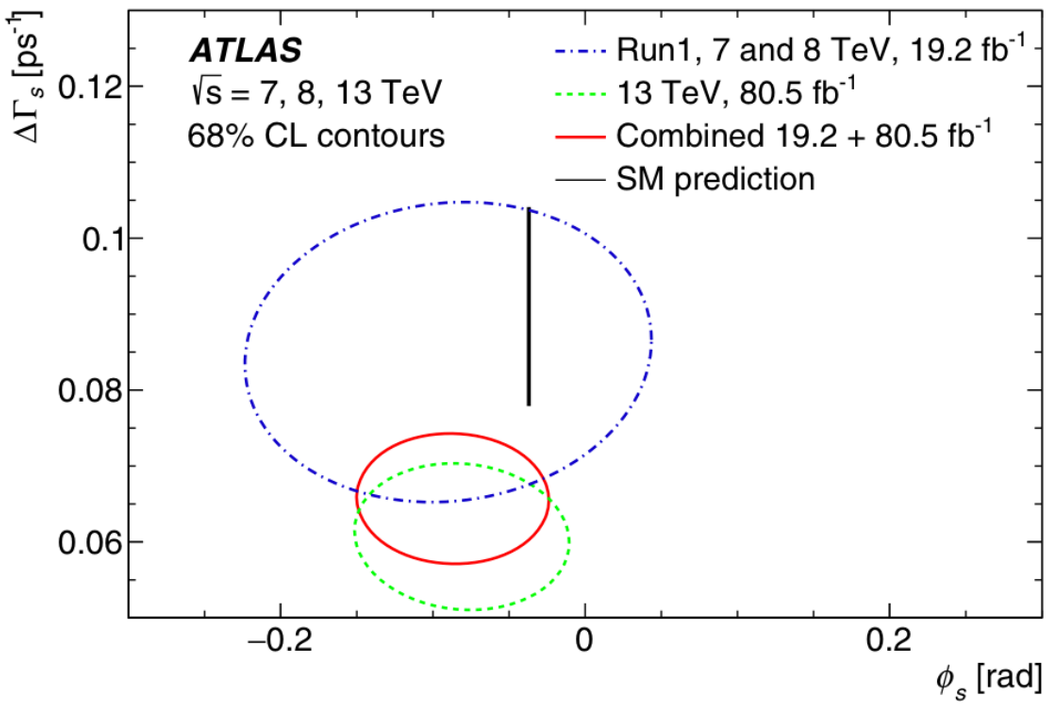

# Comparisons

- HFLAV average for PDG 2021: $\phi_s = -0.050 \pm 0.019$ rad.

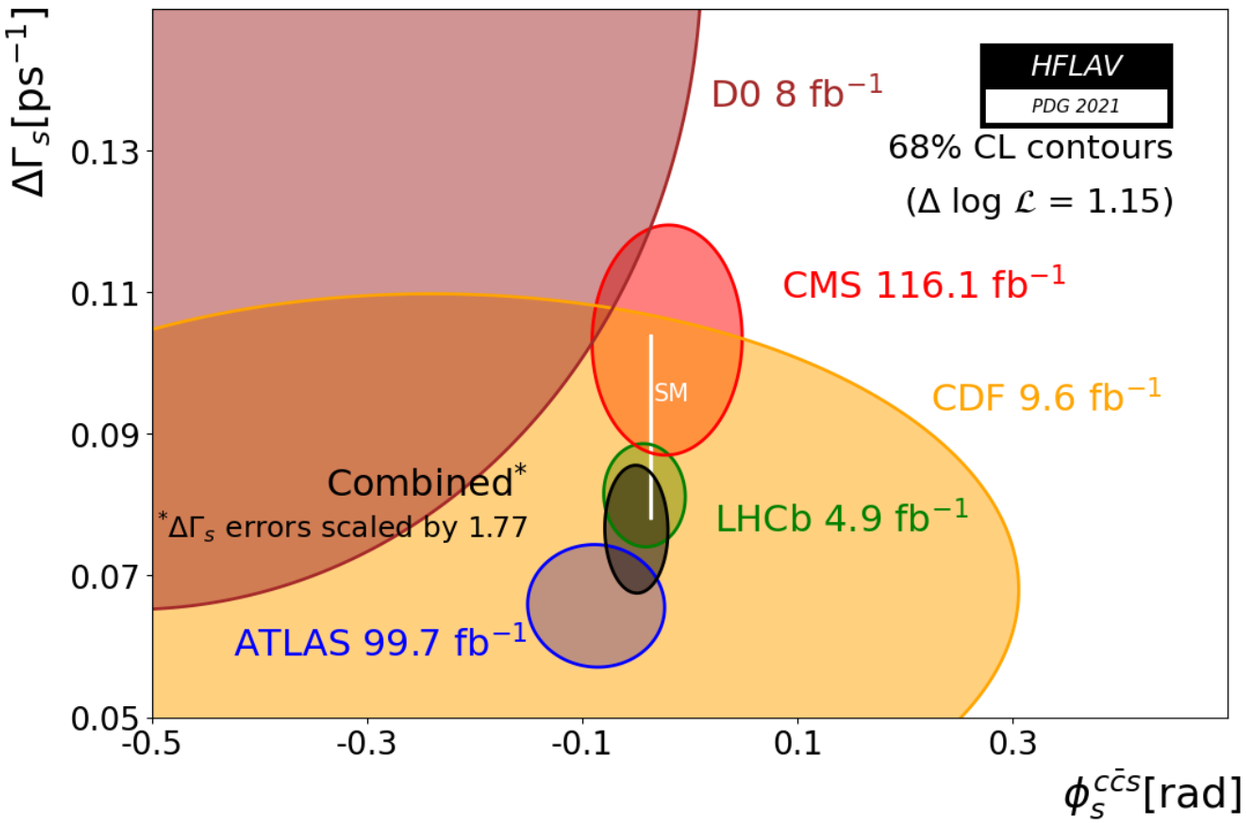


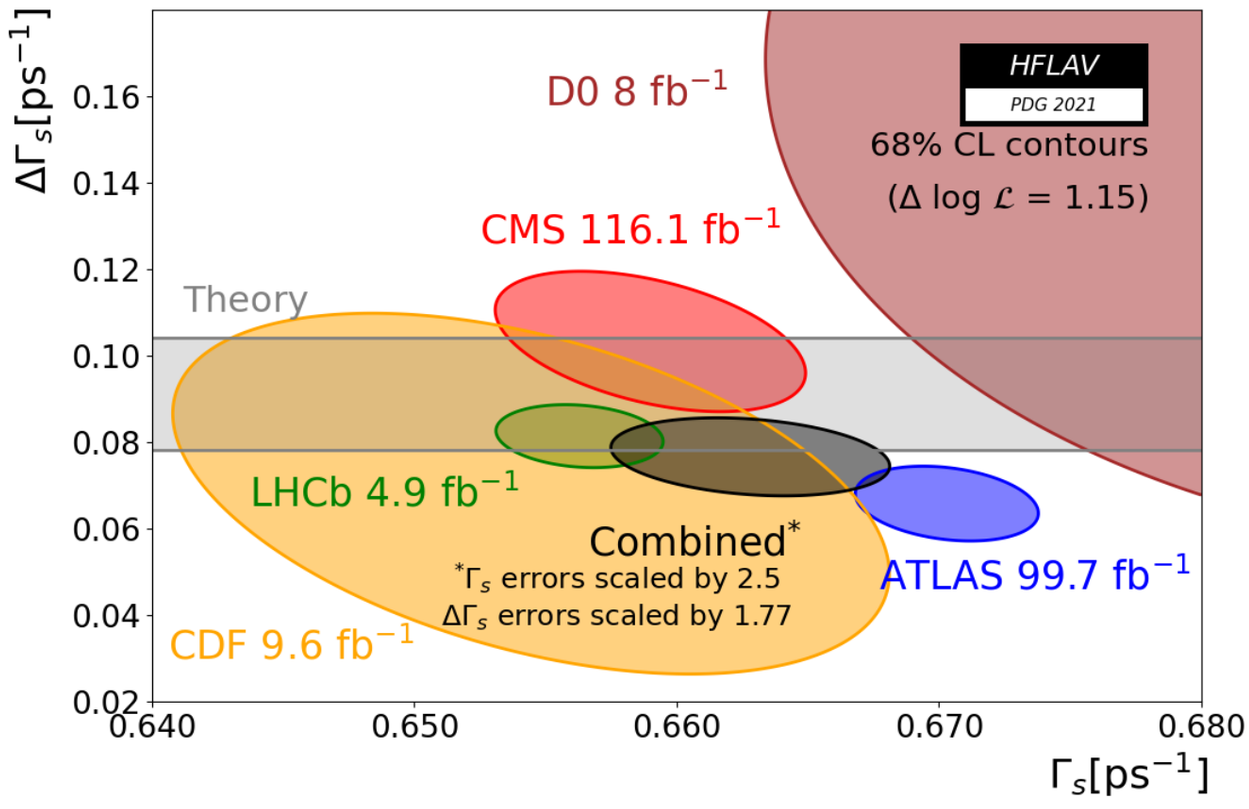

# Summary

- Analysis of di-charmonium events:
  - A broad structure at lower mass and a resonance around **6.9 GeV** are observed in the di-$J/\psi$ channel.
  - A significant of $4.6\sigma$ is observed in the $J/\psi + \psi(2S)$channel with a model of an enhancement at about 6.9 GeV plus a standalone peak.
- Measurement of CP-violation phase:
  - The measured values of physical parameters are consistent with the SM values.
  - Working with full Run2 data to improve precision.

Thanks!

# BACKUP

# Introduction

- The quark model was proposed by Gell-Mann and Zweig sixty years ago

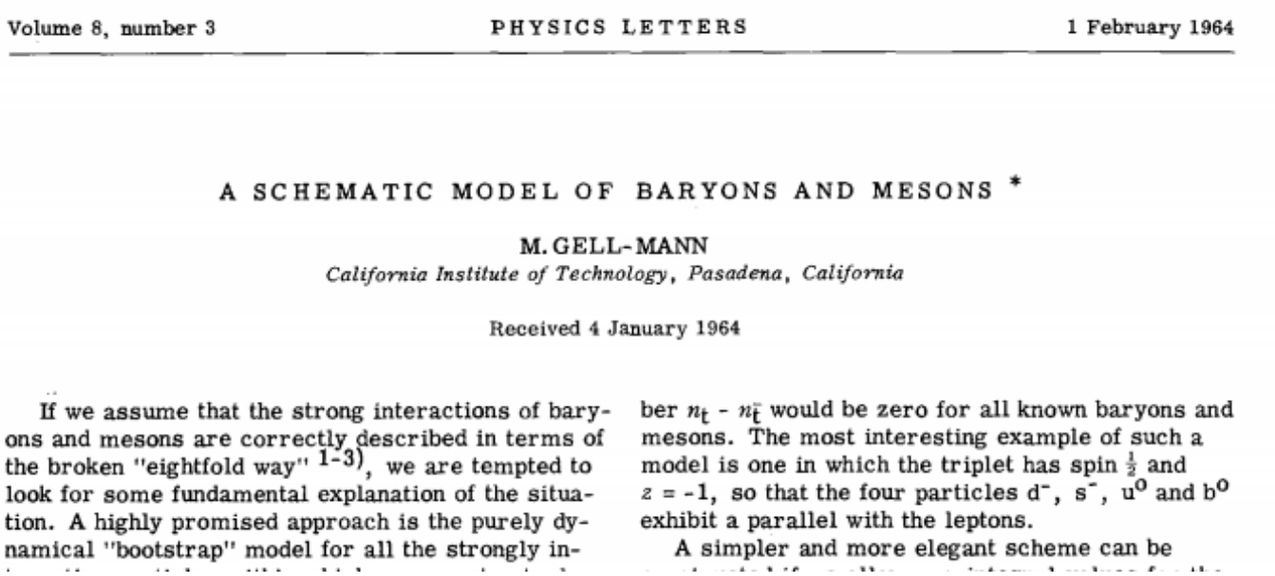

Volume 8, number 3 PHYSICS LETTERS 1 February 1964

A SCHEMATIC MODEL OF BARYONS AND MESONS *

M. GELL-MANN
*California Institute of Technology, Pasadena, California*

Received 4 January 1964

If we assume that the strong interactions of baryons and mesons are correctly described in terms of the broken "eightfold way" [1-3], we are tempted to look for some fundamental explanation of the situation. A highly promised approach is the purely dynamical "bootstrap" model for all the strongly in-

ber $n_t - n_{\bar{t}}$ would be zero for all known baryons and mesons. The most interesting example of such a model is one in which the triplet has spin $\frac{1}{2}$ and $z = -1$, so that the four particles $d^-$, $s^-$, $u^0$ and $b^0$ exhibit a parallel with the leptons.

A simpler and more elegant scheme can be

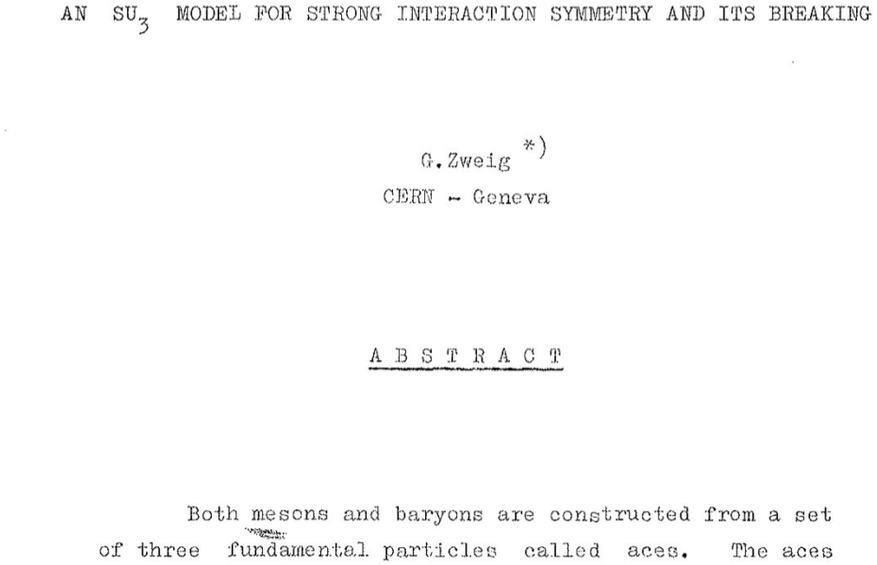

AN $SU_3$ MODEL FOR STRONG INTERACTION SYMMETRY AND ITS BREAKING

G. Zweig *)
CERN - Geneva

ABSTRACT

Both mesons and baryons are constructed from a set of three fundamental particles called aces. The aces

- Exotic hadrons were predicted at the same time as conventional $q\bar{q}$ mesons and $qqq$ baryons.

Glueball

Hybrid meson

Tetraquark

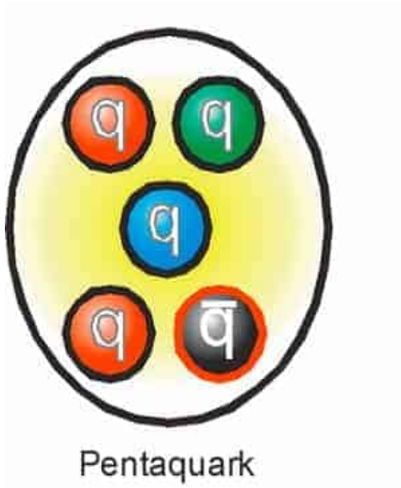


Pentaquark

# The ATLAS detector

- ATLAS (A Toroidal LHC ApparatuS) is one of the two general-purpose detectors at the Large Hadron Collider (LHC)
  - Coverage: $|\eta| < 2.5$
  - Magnetic field: 2T

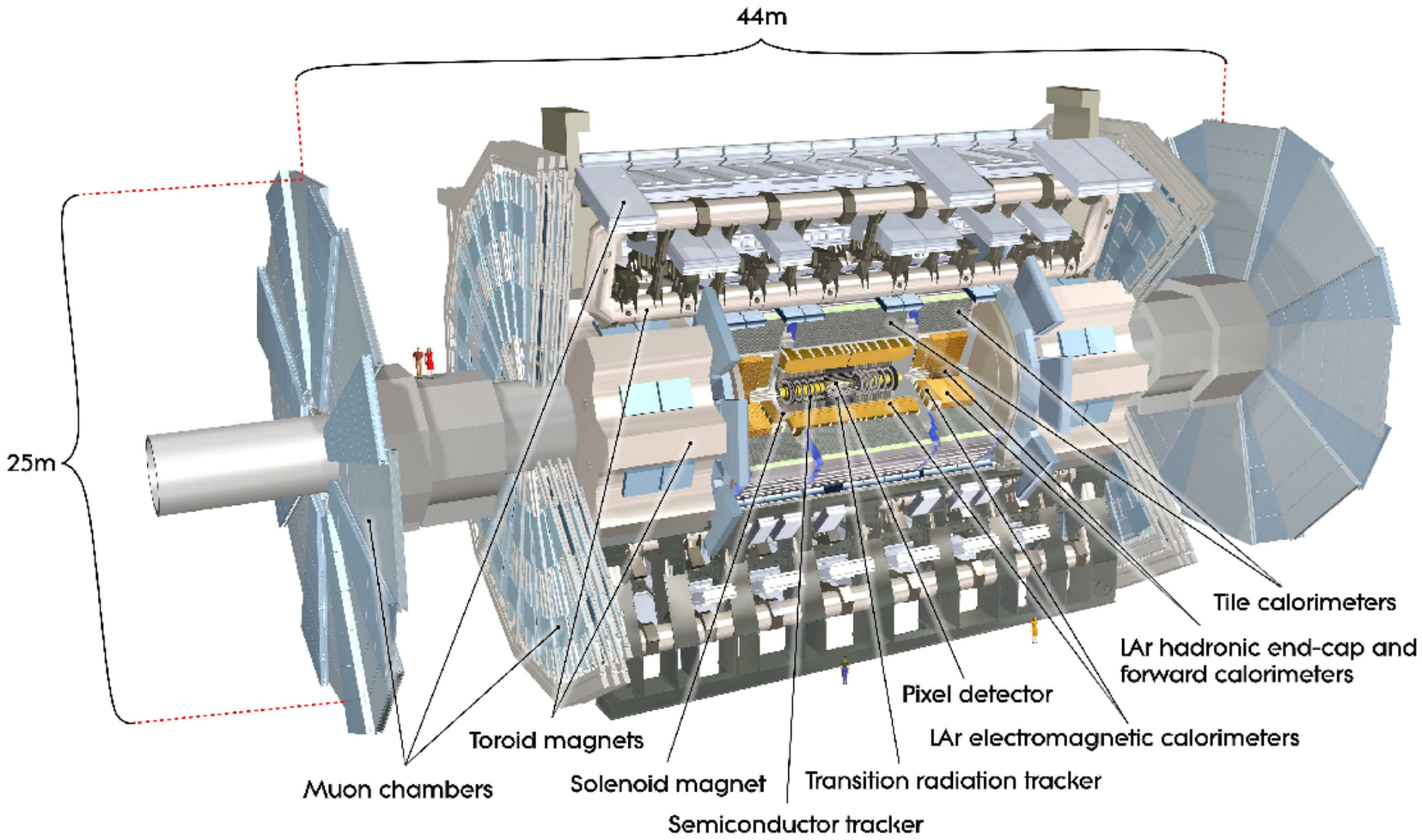

# MC samples

| Di-charmonium Process | Generator | PDF | Parton shower | Tune |
|---|---|---|---|---|
| SPS | Pythia 8.244[20] | NNPDF23LO[22] | Pythia 8.244+NNPDF23LO | A14[21] |
| DPS | Pythia 8.244 | NNPDF23LO | | A14 |
| Non-prompt | Pythia 8.244 | NNPDF23LO | | A14 |
| X(6900) | JHU[26] | CTEQ6L1[27] | | A14 |

# Functions

✦ Likelihood function:

$$\mathcal{L} = \mathcal{L}_{SR}\left(\vec{\alpha}, \vec{\beta}\right) \cdot \mathcal{L}_{CR}\left(\vec{\alpha}\right) \cdot \prod_{j=1}^{K} G\left(\alpha'_j; \alpha_j, \sigma_j\right)$$

✦ Significance is calculated with asymptotic formula:

$$Z = \sqrt{2 \ln \frac{L(\hat{s}, \hat{\theta})}{L(s{=}0, \hat{\hat{\theta}})}}$$

# Event selection

✦ Di-muon or tri-muon triggers

✦ Baseline selections:

➡ Two positive charged muons and two negative charged muons:

- $p_T(\mu_1) > 4$, $p_T(\mu_2) > 4$, $p_T(\mu_3) > 3$, $p_T(\mu_4) > 2$ GeV
- $|\eta_{\mu_1,\,\mu_2,\,\mu_3,\,\mu_4}| < 2.5$

➡ $J/\psi$ mass window: 2.94 GeV< $m_{J/\psi}$ < 3.25 GeV ; $\psi(2S)$ mass window: $3.56 < m_{\psi} < 3.80$ GeV

➡ Loose vertex cuts:

- Vertex fit quality of $4\mu$ candidate: $\chi^2_{4\mu}/N < 40$
- Vertex fit quality of $J/\psi$ and $\psi(2S)$: $\chi^2_{di-\mu}/N < 100$

# CPV — flavour tagging

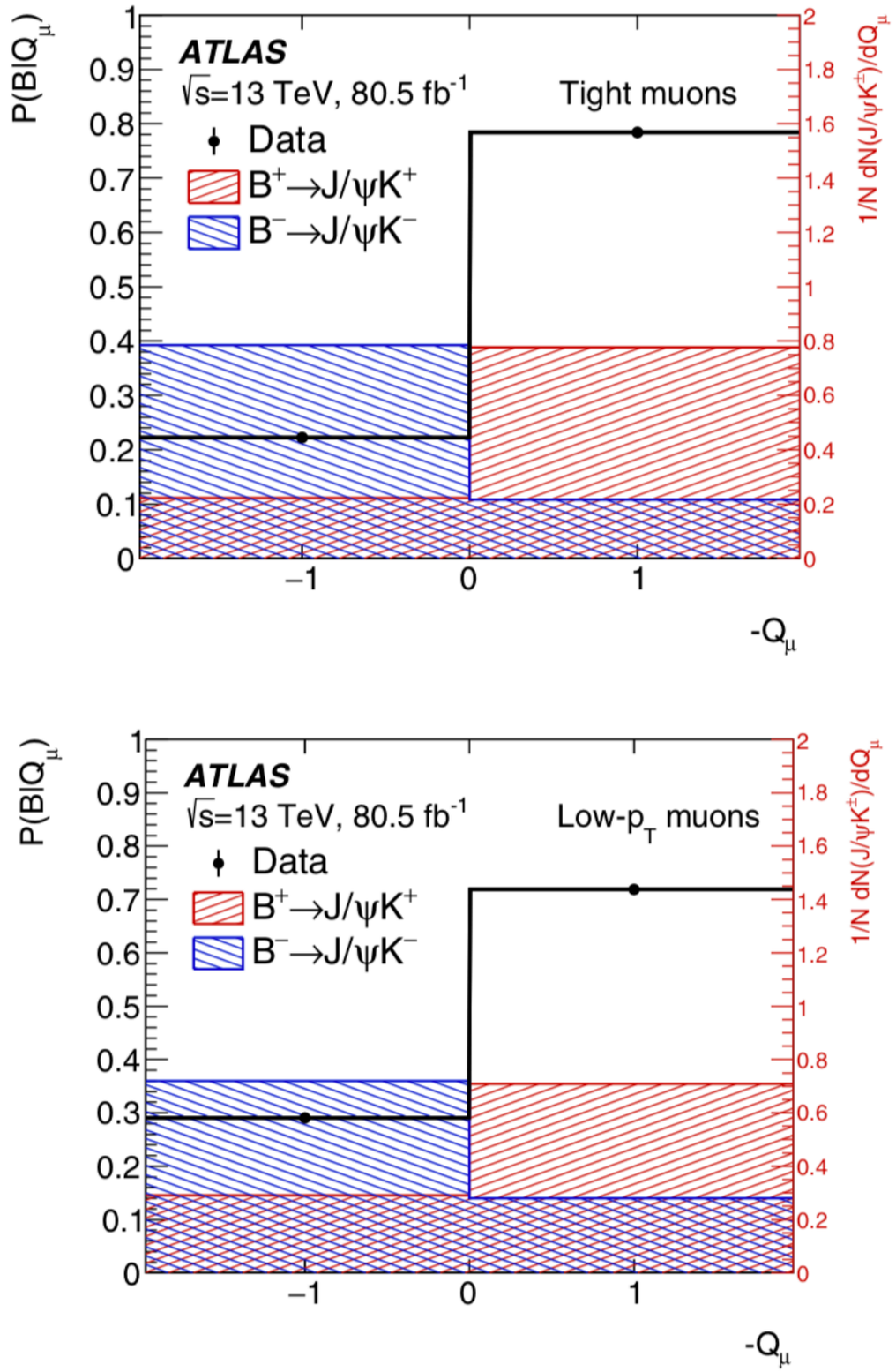


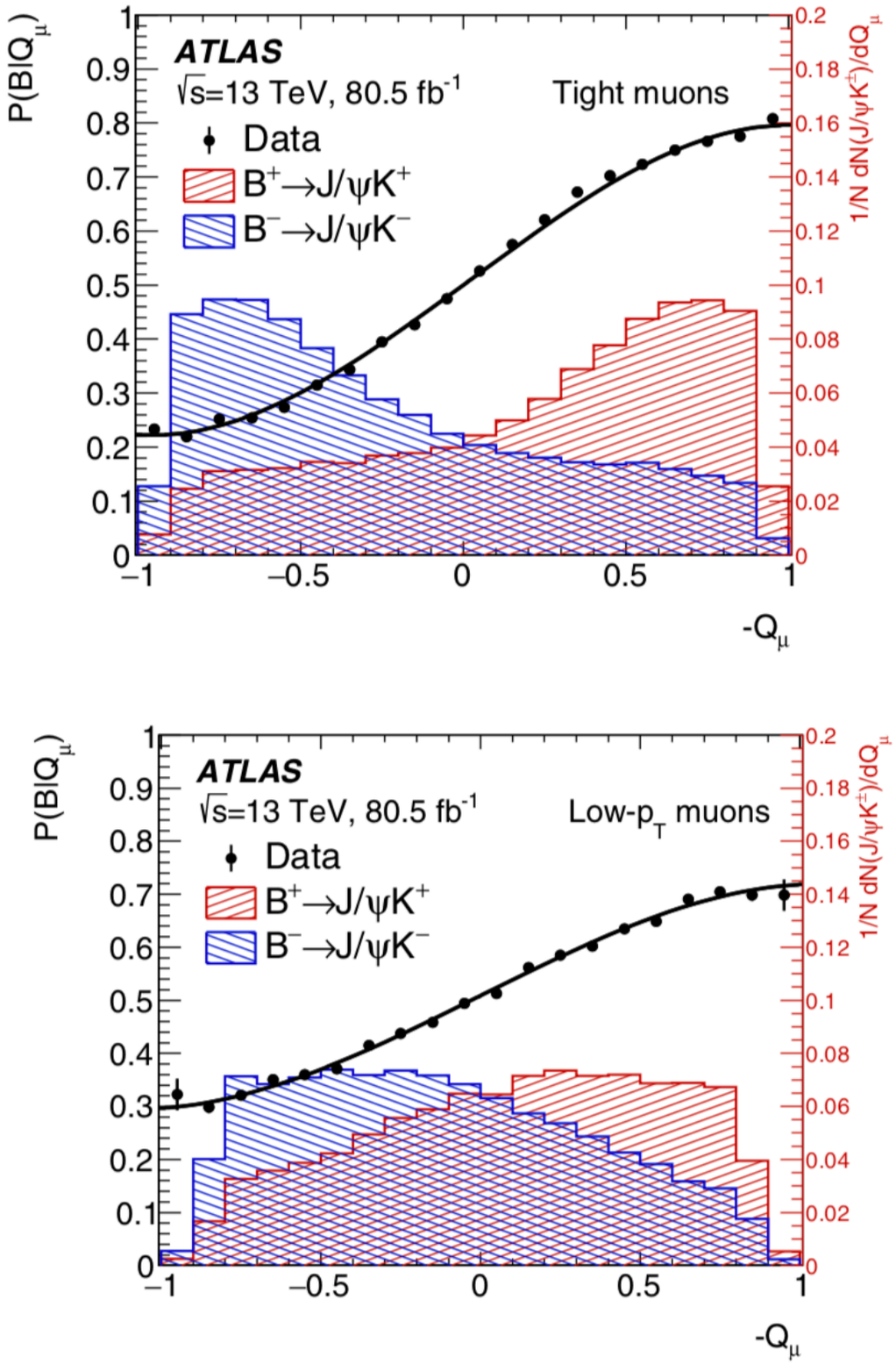

# CPV — flavour tagging

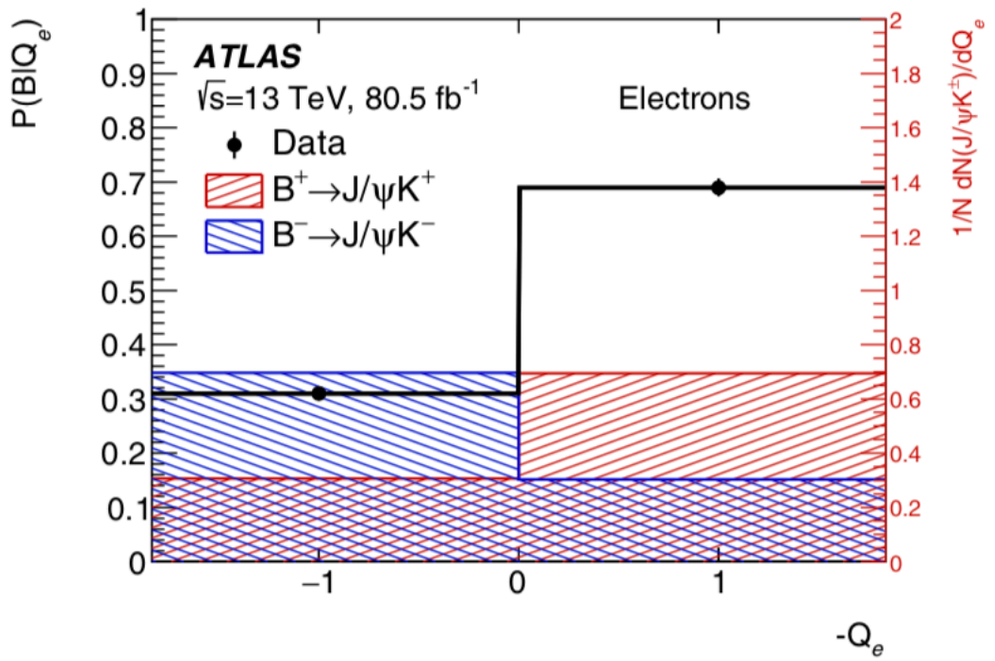


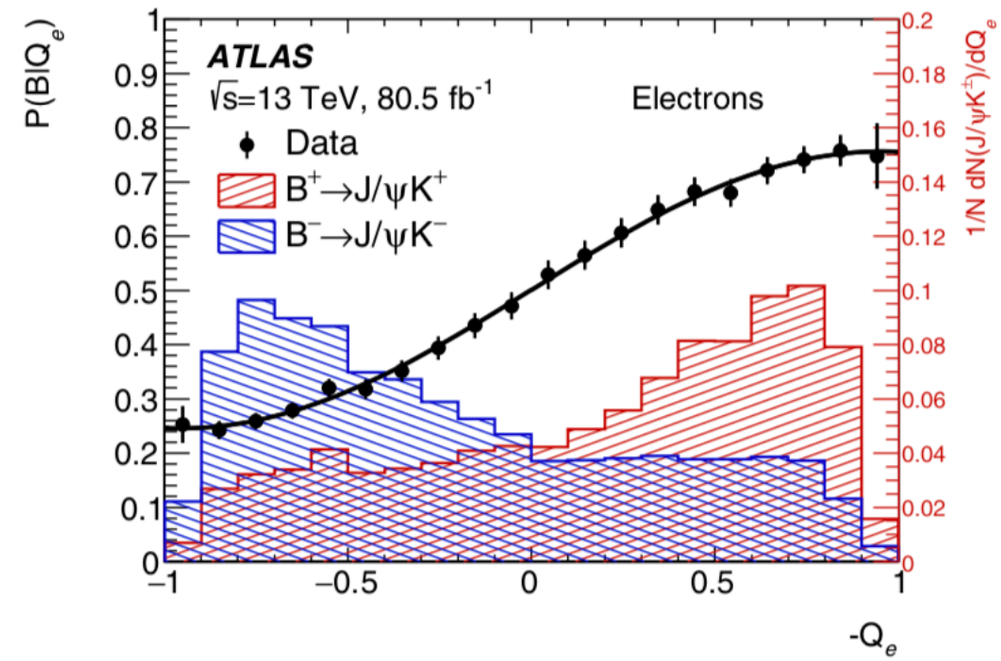


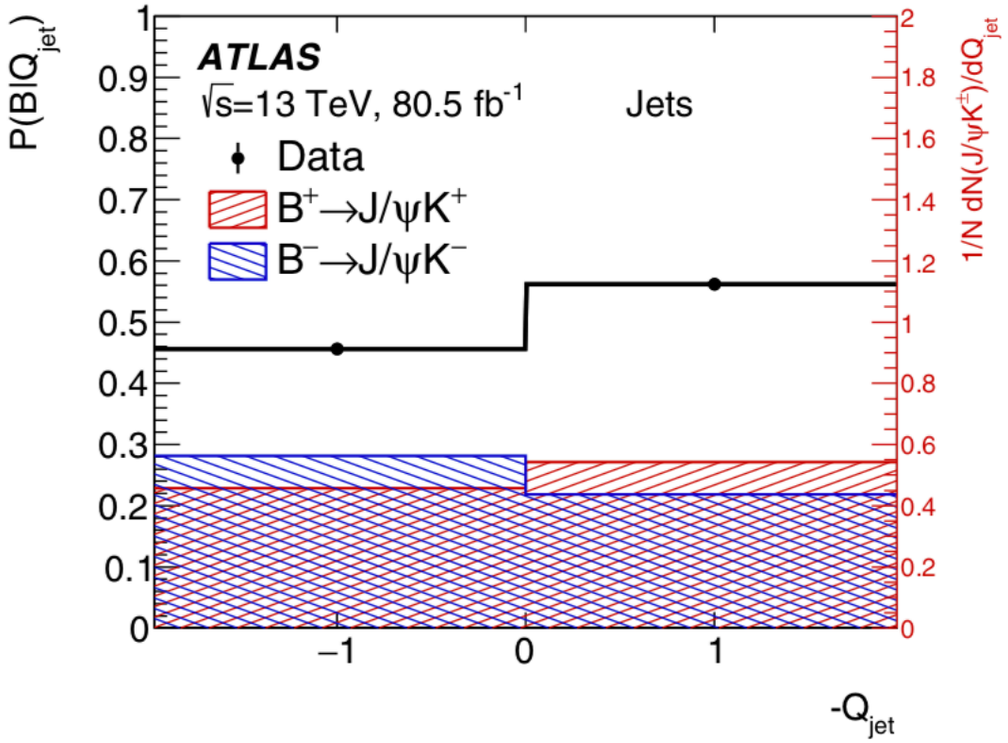


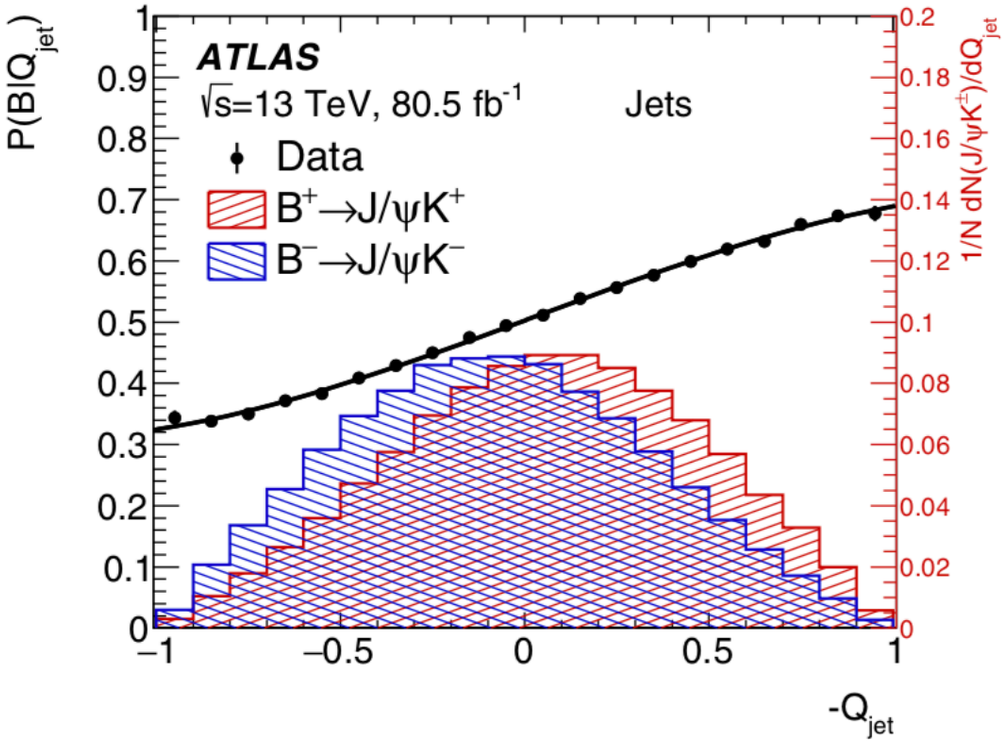

# CPV — parameters

**Table 4** The ten time-dependent functions, $O^{(k)}(t)$ and the functions of the transversity angles $g^{(k)}(\theta_T, \psi_T, \phi_T)$. The amplitudes $|A_0(0)|^2$ and $|A_\parallel(0)|^2$ are for the $CP$-even components of the $B_s^0 \to J/\psi\phi$ decay, $|A_\perp(0)|^2$ is the $CP$-odd amplitude; they have corresponding strong phases $\delta_0$, $\delta_\parallel$ and $\delta_\perp$. By convention, $\delta_0$ is set to be zero. The $S$-wave amplitude $|A_S(0)|^2$ gives the fraction of $B_s^0 \to J/\psi K^+K^-(f_0)$ and has a related strong phase $\delta_S$. The factor $\alpha$ is described in the text of Sect. 5.1. The $\pm$ and $\mp$ terms denote two cases: the upper sign describes the decay of a meson that was initially a $B_s^0$ meson, while the lower sign describes the decays of a meson that was initially $\bar{B}_s^0$

| $k$ | $O^{(k)}(t)$ | $g^{(k)}(\theta_T, \psi_T, \phi_T)$ |
|---|---|---|
| 1 | $\frac{1}{2}\lvert A_0(0)\rvert^2 \left[(1+\cos\phi_s)\,e^{-\Gamma_L^{(s)}t} + (1-\cos\phi_s)\,e^{-\Gamma_H^{(s)}t} \pm 2e^{-\Gamma_s t}\sin(\Delta m_s t)\sin\phi_s\right]$ | $2\cos^2\psi_T(1-\sin^2\theta_T\cos^2\phi_T)$ |
| 2 | $\frac{1}{2}\lvert A_\parallel(0)\rvert^2 \left[(1+\cos\phi_s)\,e^{-\Gamma_L^{(s)}t} + (1-\cos\phi_s)\,e^{-\Gamma_H^{(s)}t} \pm 2e^{-\Gamma_s t}\sin(\Delta m_s t)\sin\phi_s\right]$ | $\sin^2\psi_T(1-\sin^2\theta_T\sin^2\phi_T)$ |
| 3 | $\frac{1}{2}\lvert A_\perp(0)\rvert^2 \left[(1-\cos\phi_s)\,e^{-\Gamma_L^{(s)}t} + (1+\cos\phi_s)\,e^{-\Gamma_H^{(s)}t} \mp 2e^{-\Gamma_s t}\sin(\Delta m_s t)\sin\phi_s\right]$ | $\sin^2\psi_T\sin^2\theta_T$ |
| 4 | $\frac{1}{2}\lvert A_0(0)\rvert\lvert A_\parallel(0)\rvert\cos\delta_{\parallel} \left[(1+\cos\phi_s)\,e^{-\Gamma_L^{(s)}t} + (1-\cos\phi_s)\,e^{-\Gamma_H^{(s)}t} \pm 2e^{-\Gamma_s t}\sin(\Delta m_s t)\sin\phi_s\right]$ | $\frac{1}{\sqrt{2}}\sin 2\psi_T\sin^2\theta_T\sin 2\phi_T$ |
| 5 | $\lvert A_\parallel(0)\rvert\lvert A_\perp(0)\rvert\left[\frac{1}{2}(e^{-\Gamma_L^{(s)}t} - e^{-\Gamma_H^{(s)}t})\cos(\delta_\perp-\delta_{\parallel})\sin\phi_s \pm e^{-\Gamma_s t}(\sin(\delta_\perp-\delta_\parallel)\cos(\Delta m_s t)\right.$ $\left.-\cos(\delta_\perp-\delta_\parallel)\cos\phi_s\sin(\Delta m_s t))\right]$ | $-\sin^2\psi_T\sin 2\theta_T\sin\phi_T$ |
| 6 | $\lvert A_0(0)\rvert\lvert A_\perp(0)\rvert\left[\frac{1}{2}(e^{-\Gamma_L^{(s)}t} - e^{-\Gamma_H^{(s)}t})\cos\delta_\perp\sin\phi_s \pm e^{-\Gamma_s t}(\sin\delta_\perp\cos(\Delta m_s t) - \cos\delta_\perp\cos\phi_s\sin(\Delta m_s t))\right]$ | $\frac{1}{\sqrt{2}}\sin 2\psi_T\sin 2\theta_T\cos\phi_T$ |
| 7 | $\frac{1}{2}\lvert A_S(0)\rvert^2 \left[(1-\cos\phi_s)\,e^{-\Gamma_L^{(s)}t} + (1+\cos\phi_s)\,e^{-\Gamma_H^{(s)}t} \mp 2e^{-\Gamma_s t}\sin(\Delta m_s t)\sin\phi_s\right]$ | $\frac{2}{3}\left(1-\sin^2\theta_T\cos^2\phi_T\right)$ |
| 8 | $\alpha\lvert A_S(0)\rvert\lvert A_\parallel(0)\rvert\left[\frac{1}{2}(e^{-\Gamma_L^{(s)}t} - e^{-\Gamma_H^{(s)}t})\sin(\delta_\parallel-\delta_S)\sin\phi_s \pm e^{-\Gamma_s t}(\cos(\delta_\parallel-\delta_S)\cos(\Delta m_s t)\right.$ $\left.-\sin(\delta_\parallel-\delta_S)\cos\phi_s\sin(\Delta m_s t))\right]$ | $\frac{1}{3}\sqrt{6}\sin\psi_T\sin^2\theta_T\sin 2\phi_T$ |
| 9 | $\frac{1}{2}\alpha\lvert A_S(0)\rvert\lvert A_\perp(0)\rvert\sin(\delta_\perp-\delta_S)\left[(1-\cos\phi_s)\,e^{-\Gamma_L^{(s)}t} + (1+\cos\phi_s)\,e^{-\Gamma_H^{(s)}t} \mp 2e^{-\Gamma_s t}\sin(\Delta m_s t)\sin\phi_s\right]$ | $\frac{1}{3}\sqrt{6}\sin\psi_T\sin 2\theta_T\cos\phi_T$ |
| 10 | $\alpha\lvert A_0(0)\rvert\lvert A_S(0)\rvert\left[\frac{1}{2}(e^{-\Gamma_H^{(s)}t} - e^{-\Gamma_L^{(s)}t})\sin\delta_S\sin\phi_s \pm e^{-\Gamma_s t}(\cos\delta_S\cos(\Delta m_s t) + \sin\delta_S\cos\phi_s\sin(\Delta m_s t))\right]$ | $\frac{4}{3}\sqrt{3}\cos\psi_T\left(1-\sin^2\theta_T\cos^2\phi_T\right)$ |

# CPV — fit results

| Parameter | Value | Statistical uncertainty | Systematic uncertainty |
|---|---|---|---|
| $\phi_s$ [rad] | $-0.081$ | 0.041 | 0.022 |
| $\Delta\Gamma_s$ [ps$^{-1}$] | 0.0607 | 0.0047 | 0.0043 |
| $\Gamma_s$ [ps$^{-1}$] | 0.6687 | 0.0015 | 0.0022 |
| $\lvert A_{\parallel}(0)\rvert^2$ | 0.2213 | 0.0019 | 0.0023 |
| $\lvert A_0(0)\rvert^2$ | 0.5131 | 0.0013 | 0.0038 |
| $\lvert A_S(0)\rvert^2$ | 0.0321 | 0.0033 | 0.0046 |
| $\delta_\perp - \delta_S$ [rad] | $-0.25$ | 0.05 | 0.04 |
| Solution (a) | | | |
| $\delta_\perp$ [rad] | 3.12 | 0.11 | 0.06 |
| $\delta_{\parallel}$ [rad] | 3.35 | 0.05 | 0.09 |
| Solution (b) | | | |
| $\delta_\perp$ [rad] | 2.91 | 0.11 | 0.06 |
| $\delta_{\parallel}$ [rad] | 2.94 | 0.05 | 0.09 |

# CPV — systematics

**Table 5** Summary of systematic uncertainties assigned to the physical parameters of interest

| | $\phi_s$ ($10^{-3}$ rad) | $\Delta\Gamma_s$ ($10^{-3}$ ps$^{-1}$) | $\Gamma_s$ ($10^{-3}$ ps$^{-1}$) | $\lvert A_\parallel(0)\rvert^2$ ($10^{-3}$) | $\lvert A_0(0)\rvert^2$ ($10^{-3}$) | $\lvert A_S(0)\rvert^2$ ($10^{-3}$) | $\delta_\perp$ ($10^{-3}$ rad) | $\delta_\parallel$ ($10^{-3}$ rad) | $\delta_\perp - \delta_S$ ($10^{-3}$ rad) |
|---|---|---|---|---|---|---|---|---|---|
| Tagging | 19 | 0.4 | 0.3 | 0.2 | 0.2 | 1.1 | 17 | 19 | 2.3 |
| ID alignment | 0.8 | 0.2 | 0.5 | $< 0.1$ | $< 0.1$ | $< 0.1$ | 11 | 7.2 | $< 0.1$ |
| Acceptance | 0.5 | 0.3 | $< 0.1$ | 1.0 | 0.9 | 2.9 | 37 | 64 | 8.6 |
| Time efficiency | 0.2 | 0.2 | 0.5 | $< 0.1$ | $< 0.1$ | 0.1 | 3.0 | 5.7 | 0.5 |
| Best candidate selection | 0.4 | 1.6 | 1.3 | 0.1 | 1.0 | 0.5 | 2.3 | 7.0 | 7.4 |
| Background angles model | | | | | | | | | |
| Choice of fit function | 2.5 | $< 0.1$ | 0.3 | 1.1 | $< 0.1$ | 0.6 | 12 | 0.9 | 1.1 |
| Choice of $p_{\mathrm{T}}$ bins | 1.3 | 0.5 | $< 0.1$ | 0.4 | 0.5 | 1.2 | 1.5 | 7.2 | 1.0 |
| Choice of mass window | 9.3 | 3.3 | 0.2 | 0.4 | 0.8 | 0.9 | 17 | 8.6 | 6.0 |
| Choice of sidebands intervals | 0.4 | 0.1 | 0.1 | 0.3 | 0.3 | 1.3 | 4.4 | 7.4 | 2.3 |
| Dedicated backgrounds | | | | | | | | | |
| $B_d^0$ | 2.6 | 1.1 | $< 0.1$ | 0.2 | 3.1 | 1.5 | 10 | 23 | 2.1 |
| $\Lambda_b$ | 1.6 | 0.3 | 0.2 | 0.5 | 1.2 | 1.8 | 14 | 30 | 0.8 |
| Alternate $\Delta m_s$ | 1.0 | $< 0.1$ | $< 0.1$ | $< 0.1$ | $< 0.1$ | $< 0.1$ | 15 | 4.0 | $< 0.1$ |
| Fit model | | | | | | | | | |
| Time res. sig frac | 1.4 | 1.1 | 0.5 | 0.5 | 0.6 | 0.8 | 12 | 30 | 0.4 |
| Time res. $p_{\mathrm{T}}$ bins | 0.7 | 0.5 | 0.8 | 0.1 | 0.1 | 0.1 | 2.2 | 14 | 0.7 |
| $S$-wave phase | 0.3 | $< 0.1$ | $< 0.1$ | $< 0.1$ | $< 0.1$ | 0.2 | 8.0 | 15 | 37 |
| Fit bias | 5.7 | 1.3 | 1.2 | 1.3 | 0.4 | 1.1 | 3.3 | 19 | 0.3 |
| Total | 22 | 4.3 | 2.2 | 2.3 | 3.8 | 4.6 | 55 | 88 | 39 |